SURFACE PROPERTIES AND TEXTURE OF CHRYSOTILES

by

J. J. FRIPIAT* and M. DELLA FAILLE†

Laboratoire de Physico-Chimie Minérale, Institut Agronomique,
Université de Louvain, Heverlee-Louvain (Belgium)

ABSTRACT

NITROGEN surface areas and pore-size distribution curves of various chrysotiles have been measured using a continuous flow method. A model founded on a hexagonal close packing of fibers has been adjusted to fit the frequency distribution curve of the fiber outside diameters obtained from electron micrographs. From this model, theoretical distribution functions of the surface area versus the pore diameter were computed and compared to the experimental data. For one fiber only (i.e. Coalinga chrysotile), the good agreement between the computed and experimental data allows one to conclude that the external pores (between the fibers) and the internal pores (within the fibers) are free from any amorphous material. For the other studied chrysotiles, the degree of filling of the pore system by amorphous materials was always higher than 50%. Under these conditions, hydration water cannot be removed unless the samples are pretreated in the 300°–400°C temperature range. On the contrary, water is driven off from the "clean" Coalinga fibers at temperatures lower than 100°C. Surface area measurements derived from water-adsorption isotherms correspond to those obtained with nitrogen after the hydration water has been removed.

INTRODUCTION

THE early application of electron microscopy to the study of chrysotiles had suggested fibers having an internal porous structure (Turkevich and Hillier, 1949). The relationships between structure and morphology were emphasized in the following years (Noll and Kircher, 1950, 1951, 1952) and consequently problems concerning the degree of filling of the void spaces were invoked. Young and Healey (1954), Healey and Young (1954) had shown that two kinds of surfaces might be distinguished. Internal pores seemed available to small polar molecules such as H_2O but not to N_2, unless dehydrated at rather high temperature. External pores between the fibers were considered as partially available to nitrogen. These assumptions were founded on the observation that removing water at about 400°C increases the surface area determined with N_2 to a value equivalent to that obtained with H_2O.

* The University of Louvain and M.R.A.C., Tervuren (Belgium).
† Eternit S.A., Kapelle-op-den-Bos (Belgium).

https://doi.org/10.1346/CCMN.1967.0150134 Published online by Cambridge University Press

Pundsack (1956, 1961) suggested that the accessibility of external surfaces was not as complete as claimed by Young and Healey since mechanical treatment noticeably affects the B.E.T. measurements. Moreover, the apparent density deduced from water adsorption isotherms was close to the theoretical value. It was therefore concluded that the external pores (between fibers) as well as the internal pores (within individual fibers) are filled with materials of chemical composition similar to that of the bulk. In the pore-size distribution curves computed from the H_2O adsorption isotherms, two maxima were observed at 16 Å and 13 Å. They were assigned to the external pores and to the internal cylindrical pores respectively. Bates (1959), Bates and Comer (1959) tried to explain the divergent observations of Pundsack and of Young and Healey, assuming that the material filling the internal pores is a good water adsorbent.

Maser, Rice, and Klug (1960) were able to prepare sections of chrysotile fibers perpendicular to their axis. The electron micrographs showed clearly the existence of internal cylindrical pores but did not permit any conclusion upon the degree of filling. In order to explain the fiber habits usually observed on electron micrographs, Whittaker (1957) calculated the screening effect of eventual amorphous materials on the scattering of electrons. The scattering distribution curve across the fiber was not appreciably modified whether or not amorphous substances are present in the internal pore.

Facing these divergent interpretations, the present contribution aims to study systematically the surface properties of chrysotiles and, especially, to analyse carefully numerous pore-size distribution curves computed from N_2 adsorption isotherms after various thermal pretreatments. Recent development of a rapid continuous flow method (Cahen *et al.*, 1965) for measuring pore-size distributions has made this work possible. Moreover, the results obtained with N_2 have been compared with those obtained with H_2O. The conclusions were checked with measurements carried out on electron micrographs.

PROCEDURES

Chrysotile Samples

The raw material was washed with water on a 400-mesh sieve. Fibers not smaller than 2 mm were separated by elutriation on a 16-mesh sieve. The origin and the structure formulae of the samples studied in this work are shown in Table 1.

The X-ray diffraction diagrams as well as the D.T.A. curves fit very well the usual patterns described for chrysotiles. Typical T.G.A. curves are shown in Fig. 1. The weight loss obtained on calcining the samples occurs in two steps, below and above 450°C respectively. Above 450°C, the weight loss corresponds to the removal of 6.5 to 7×10^{-3} H_2O mole per gram, in approximate agreement with the theoretical water content, i.e. 7.5×10^{-3} H_2O mole per gram. The weight loss of a few per cent occurring below 450°C is assumed

https://doi.org/10.1346/CCMN.1967.0150134 Published online by Cambridge University Press

TABLE 1.—ORIGINS AND STRUCTURAL FORMULAE OF CHRYSOTILES

Fiber	Origin	Structure formulae $4M^{IV}\ 6M^{VI}\ O_{10}\ (OH)_8$				
		Tetrahedral layer (M^{IV})		Octahedral layer (M^{VI})		
		Si^{4+}	Al^{3+}	Mg^{2+}	Fe^{3+}	Al^{3+}
J.M.	Jeffrey mines, Canada	3.913	0.0747	5.775	0.1915	—
Russian	Oural, S.S.S.R.	3.9415	0.0585	5.5626	0.2824	0.155
Corsica	Canari mines, Corsica	3.6712	0.2076	5.757	0.243	—
Cassiar	Bell Asbestos Mine, Vancouver, Canada	3.887	0.101	5.88	0.123	—
Coalinga	California	3.818	0.182	5.621	0.146	0.407
Arizona	Arizona	3.975	0.028	5.929	0.052	—

to represent the removal of hydration water either from internal or external pores. In order to investigate the effect of hydration water on surface properties, thermal pretreatments were carried out below 450°C. The samples were heated overnight in an oven at 100°, 200°, 300° and 400°C and carefully protected against rehydration until use. In a few cases, the temperature was increased to 650°C to produce a complete dehydroxylation. The changes in morphology and pore structure of the "thermally damaged materials" have been reported elsewhere (della Faille, De Kimpe, and Fripiat, 1966).

Pore-size Distribution Curves

In order to obtain a statistically significant number of experimental data, a rapid and continuous flow method was set up for determining nitrogen desorption isotherms (Cahen *et al.*, 1965). This technique involves passing a mixture of 15–20% nitrogen in helium through the sample cooled in liquid nitrogen at a total pressure of 4000 to 5000 mm of Hg, causing the N_2 partial pressure to approach its liquefaction pressure and nitrogen to be adsorbed. By lowering then the total pressure in a continuous and steady way, the partial pressure decreases, the adsorbed gas is progressively desorbed and the amount of N_2 evolved is recorded as a function of the pressure. The continuous recording of a desorption isotherm requires a time of 1 to 3 hours, according to the nature of the sample, instead of days, with a conventional volumetric apparatus. The desorption diagram which gives the volume of nitrogen desorbed with respect to the nitrogen partial pressure is transferred to the computer. The calculation program proposed by Cranston and Inkley (1957) was used. Several presentations of the results are possible: the most adequate for this work was that showing the fractional surface area (ΔS, m^2 per gram)

https://doi.org/10.1346/CCMN.1967.0150134 Published online by Cambridge University Press

developed by pores having diameters between Φ and $\Phi + 5$ Å, Φ being progressively increased from 20 to 250 Å. Moreover, the computer provides the surface area calculated according to the B.E.T. method. The instrument developed for pore-size distribution measurements is derived from a conventional gas chromatograph equipped with thermistor catharometers and with manometers measuring pressures up to 5 atm per cm^2. The oven-dried (or calcined) samples were degassed at the pretreatment temperature by passing a slow flow of helium (30 ml per min) overnight.

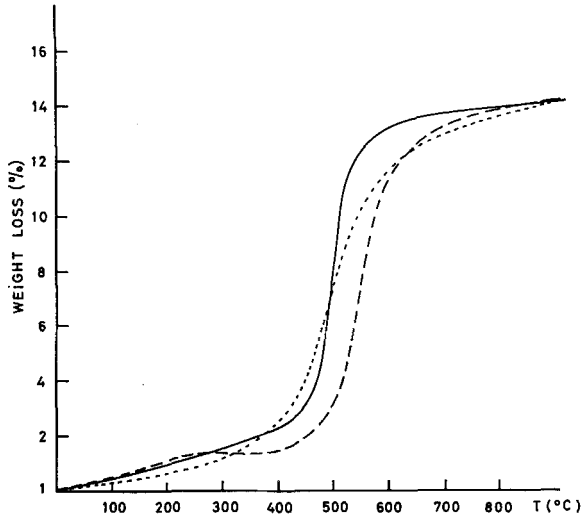


FIG. 1. Weight loss against temperature of several chrysotile samples. Solid line: J.M.; broken line: Russian; dashed line: Corsica.

Water Adsorption Isotherms

Water adsorption isotherms were obtained using a technique described by Pundsack (1961). Samples, oven-dried at 300°C and carefully protected against atmospheric moisture, were introduced in long glass tubes, immersed in a constant temperature bath maintained at 23°C ± 0.1. Each tube contained H_2O–H_2SO_4 mixtures of known water relative pressures, covering the range $0.145 < P/P_0 < 0.895$. The adsorption isotherm is obtained by weighing each sample when the equilibrium is reached, i.e. after 10–15 days. In a few cases the results were compared with those given by a vacuum electrobalance, operated at 23°C. The agreement was found satisfactory. The pretreatment temperature of 300°C was chosen in order to insure the removal of hydration water, as shown further. The surface area available to H_2O was determined by the B.E.T. method, assuming the packing of physically adsorbed water molecules to be 11 $Å^2$.

https://doi.org/10.1346/CCMN.1967.0150134 Published online by Cambridge University Press

THE THEORETICAL PORE-SIZE DISTRIBUTION

A model has been set up for the theoretical calculation of the surface area distribution as a function of the pore diameter. The following assumptions were made: (1) the fibers are arranged in hexagonal close packing to form bundles, as shown in Fig. 2, in agreement with Fankuchen and Schneider (1944); there are consequently twice as many internal as external pores; (2) the length (L) of the fiber is considered as infinite with respect to its external diameter ($2R$); (3) nitrogen cannot develop a monolayer in the regions (black in Fig. 2) where the distance between two adjacent walls is smaller than twice the molecular diameter (approximately 8 Å).

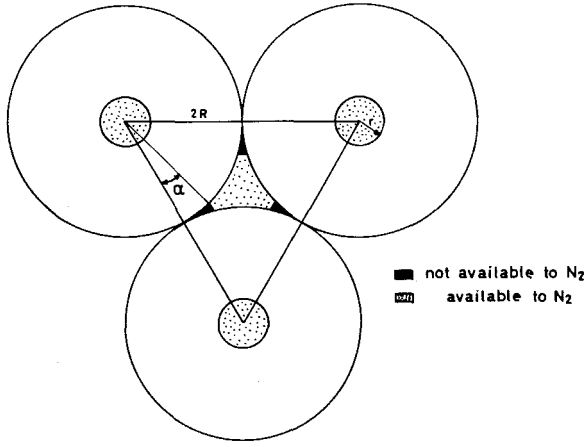


FIG. 2. Schematic representation of cylindrical hollow fibers in hexagonal close packing.

The surface area S of the external pore is then

$$S=\left(1-\frac{6\alpha}{\pi}\right)\pi RL \tag{1}$$

where

$$\sin\frac{\alpha}{2}=\sqrt{\frac{2}{R}},\quad R \text{ being expressed in Å.} \tag{2}$$

The apparent radius of a cylindrical pore of equivalent surface area would be:

$$r_{app}=\left(1-\frac{6\alpha}{\pi}\right)\frac{R}{2}. \tag{3}$$

The surface area of the internal pore is

$$s=2\pi rL. \tag{4}$$

In order to obtain the specific surface area (per gram), it is necessary to

https://doi.org/10.1346/CCMN.1967.0150134 Published online by Cambridge University Press

take into account the apparent density P_s given by

$$P_s = \frac{\pi}{2\sqrt{3}} \left(1 - \frac{r^2}{R^2}\right) \delta \tag{5}$$

where $\delta = 2.6$. Consequently the specific surface area S_0 is equal to the sum of two contributions, S^* and s^*, corresponding to the external and internal pores respectively, or:

$$S_0 = S^* + s^* \tag{6}$$

where

$$S^* = 2 \frac{1 - 6\alpha/\pi}{R(1 - r^2/R^2)\delta}$$

and

$$s^* = \frac{2r}{R^2(1 - r^2/R^2)\delta}.$$

Let f and F be the frequency distribution functions of the internal pore diameter ($2r$) and the outside fiber diameter ($2R$) respectively. Let A_i be the partial surface limited between the curve $F(R)$ and increments of 20 Å of R. Assume that r is proportional to R. It follows

$$S = \sum_i S_{0i} A_i = \sum_i (S_i^* + s_i^*) A_i \tag{7}$$

where

$$\sum_i S_i^* A_i = 2 \sum_i \frac{1 - 6\alpha_i/\pi}{R_i(1 - r_i^2/R_i^2)\delta} A_i$$

and

$$\sum_i s_i^* A_i = \sum_i \frac{2r_i}{R_i^2(1 - r_i^2/R_i^2)\delta} A_i.$$

The assumption that r is proportional to R was introduced because of the uncertainty involved in the determination of the internal pore diameter from electron micrographs. The mathematical treatment of relationship (7) was performed for various distribution curves and various R/r ratios. Figure 3 shows the F function obtained for Coalinga from measurements carried out on numerous electron micrographs, and the corresponding adjusted normal distribution. The most probable value obtained for $2R$ was 218 Å. The most probable internal diameter was estimated to 45 Å by measuring the widths of the void spaces running parallel to the axis of each individual fiber, as shown in Plate 1. The proportionality factor r_i/R_i was thus equal to 45/218 for this peculiar sample. Figure 4 shows the good agreement between the computed distribution of the specific surface area with respect to the apparent diameter $2r_{app}$ and the experimental distribution averaging data obtained after pretreatments between 100° and 400°C. The apparent diameter ($2r_{app}$) has been chosen for this representation since the calculation of the pore-size distribution from the adsorption or desorption isotherms is founded on the assumption of cylindrical pores of infinite lengths. In Table 2 the

https://doi.org/10.1346/CCMN.1967.0150134 Published online by Cambridge University Press

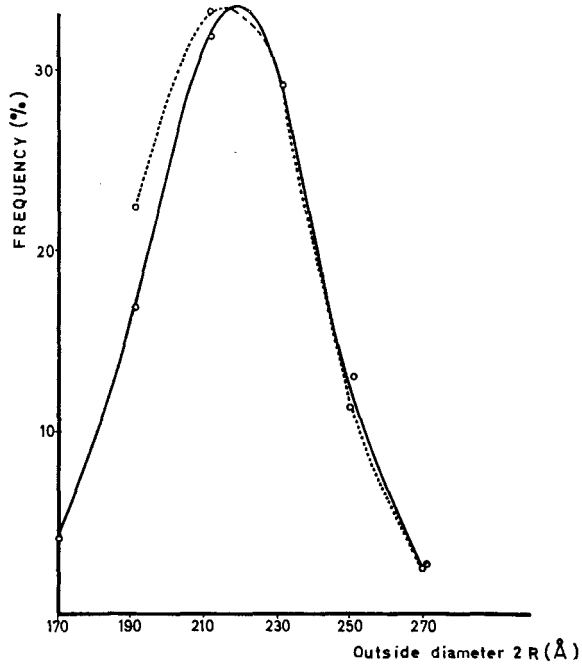


FIG. 3. Frequency distribution curves obtained by measuring the fibers outside diameters on electron micrographs (Coalinga chrysotile). Broken line: experimental distribution. Solid line: normalized distribution.

contributions of the surface areas of the external (S^*) and internal (s^*) pores are tabulated, assuming either r_i proportional to R_i or $2r = 45$ Å. The total surface areas computed in both cases are in good agreement with the B.E.T. values.

TABLE 2.—COMPUTED AND EXPERIMENTAL SURFACE AREAS OF THE COALINGA CHRYSOTILE (m^2 per gram)

r proportional to R			$2r = 45$ Å			B.E.T. after pretreatment at the indicated temperatures		
s^*	S^*	S	s^*	S^*	S	100°C	200°C	300–500°C
15.9	35.4	51.3	15.7	35.4	51.1	54.6	52.0	53.4

From the comparisons in Table 2 it may be concluded: (1) that the Coalinga sample is composed of bundles of hollow fibers arranged in close hexagonal packing, (2) and that, from a statistical viewpoint, the frequency distribution curve of $2R$ approximates a single gaussian function.

https://doi.org/10.1346/CCMN.1967.0150134 Published online by Cambridge University Press

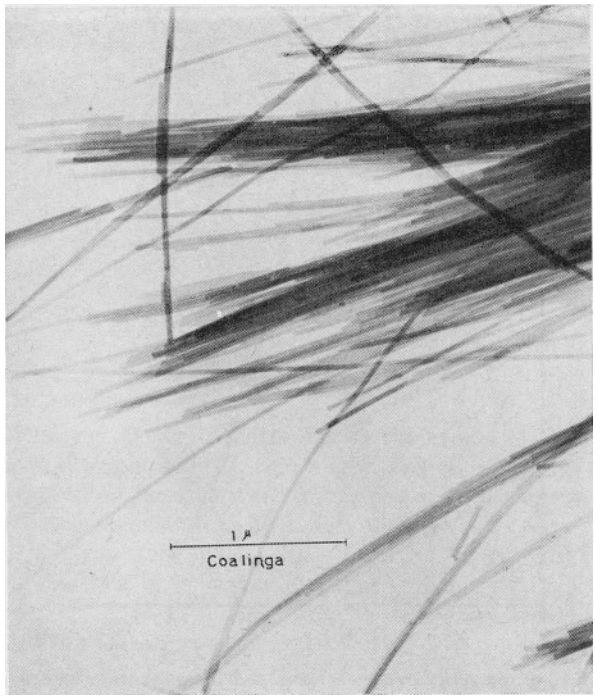


PLATE 1. Electron micrograph of Coalinga chrysotile.

An interesting consequence of the good fit between the computed and experimental distribution functions, as shown in Fig. 4, is the possibility of deriving the most probable outside diameter of individual fibers from the most probable apparent diameter $2r_{app}$, whatever the degree of filling of internal pores. In order to demonstrate this point, consider the theoretical distribution functions of Fig. 5 obtained for variable r values but with the same frequency distribution function $F(2R)$, shown in Fig. 3. The amplitude of the maximum changes greatly but it occurs always at the same apparent diameter.

SYSTEMATIC STUDY OF THE PORE-SIZE DISTRIBUTION FUNCTIONS

As shown in Figs. 6 and 7, the experimental pore-size distributions obtained for various chrysotiles have single maxima, the position and amplitude of which appear to be characteristic for each sample. This is still more apparent in Table 3, which contains the most probable apparent diameters, the outside

https://doi.org/10.1346/CCMN.1967.0150134 Published online by Cambridge University Press

diameters derived from the former through equations (2) and (3), and the B.E.T. surface areas. Some results are also given for two other fibers, i.e. Arizona (J.M. mines) and Advocate (Newfoundland). Table 3 shows the very peculiar habit of Coalinga chrysotile: the outside diameter is the highest of the series and the experimental specific surface area is almost identical to

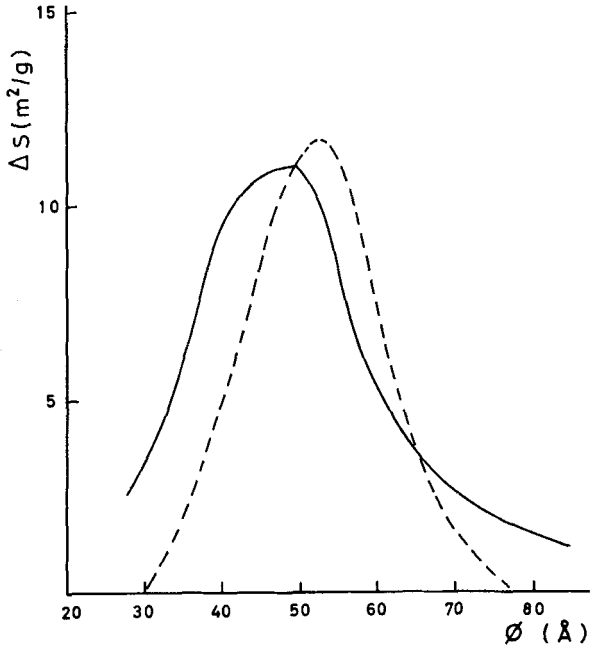


FIG. 4. Distribution functions obtained for the Coalinga chrysotile. Broken line: computed function (equation 7) assuming r_i being proportional to R_i. Solid line: experimental function averaging the results obtained after pretreatment in the 100–500°C range.

the theoretical value. This agreement is in favor of "free" porous spaces, not occluded with amorphous materials. For the other fibers, according to the previous calculations, the minimum surface areas expected from the most probable $2R$ value would be at least higher than 40 m^2/g, whatever the value of the internal pore radii. Even after pretreatment at 400°C, such surface areas have never been measured. Therefore it may be concluded that the internal or external pores contain appreciable amounts of amorphous materials. The degree of filling could be calculated if r could be determined accurately, but measuring this parameter from usual electron micrographs seems highly hazardous.

Upon increasing the pretreatment temperature, the surface areas increase, sometimes slightly, sometimes more strongly. As proposed earlier, this may

https://doi.org/10.1346/CCMN.1967.0150134 Published online by Cambridge University Press

result from removing water molecules filling partially the void spaces. However, the thermal pretreatment of Coalinga does not affect the surface area. Since the internal and external pore diameters are quite high for this fiber and the degree of filling with amorphous materials is very low, it seems

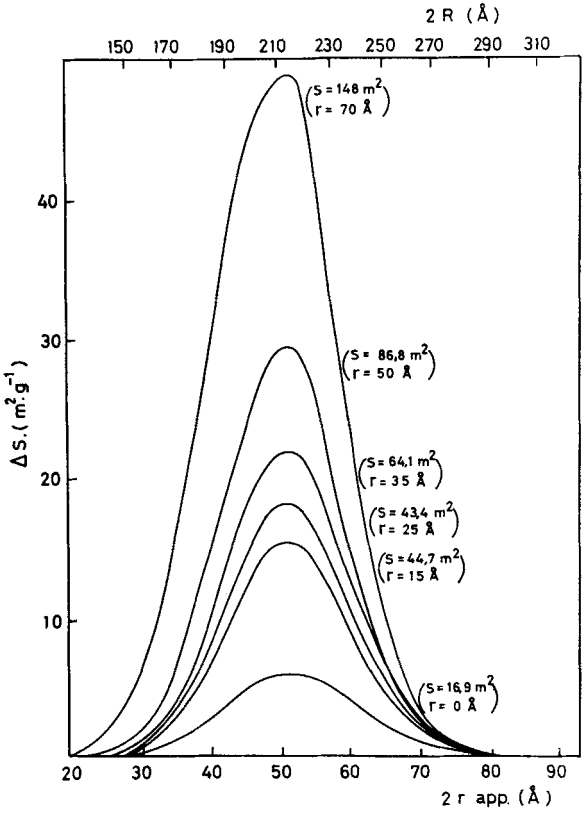


FIG. 5. Theoretical distribution functions obtained assuming the same frequency distribution function as in Fig. 3, but for variable internal pore radii (r).

appropriate to suggest that water molecules diffuse freely in the channels and that they may be removed at temperatures as low as 100°C. On the contrary, for a fiber such as Cassiar, the constancy of low surface areas at any pretreatment temperature should be explained assuming that the degree of filling by amorphous materials is quite high and that eventual hydration water molecules cannot diffuse appreciably unless high temperatures are reached. Dehydroxylation and dehydration occur then simultaneously, deeply damaging the original structure (della Faille, De Kimpe, and Fripiat, 1966).

https://doi.org/10.1346/CCMN.1967.0150134 Published online by Cambridge University Press

TABLE 3.—MAIN TEXTURAL AND SURFACE CHARACTERISTICS

Fiber	Pretreatment temperature (°C)	Most probable $2r_{app}$ (Å)	S (B.E.T.) m^2/g	Most probable outside diameter ($2R$) (Å)	Most probable outside diameter (electron micrographs) (Å)
Russian	100	27.5	13.5		
	200	32.5	14.0		
	300	27.5	21.0	156	—
	400	32.5	14.2		
	500	32.5	19.7		
		Average: 30.0 (below 500°C)			
Corsica	100	37.5	6		
	200	37.5	7.3		
	300	37.5	11.5	176	—
	400	32.5	17.0		
	500	32.5	12.2		
		Average: 37.5 (below 400°C)			
Coalinga	100	49.0	54.6		218
	200	49.0	52.0	210	220 (P)
	300–500	49.0	53.4		
		Average: 49.0			
Arizona	100–300	22.5	12.9	136	
	400–500	22.5	17.6		
		Average: 22.5			
Advocate	100–200	32.5	17.2		
	300–400	32.5	21.2	162	159 (P)
	500	32.5	21.5		
		Average: 32.5			
J.M.	100	27.5	16.6	150	160 (P)
	200	27.5	18.4		
		Average: 27.5			
Cassiar	100–200	22.5	12.0		
	300	27.5	14.3	143	
	400	27.5	12.3		
	500	27.5	10.0		
		Average: 25.0 (below 400°C)			

N.B. The most probable outside diameters computed from electron micrographs and indicated with subscripts P are due to the courtesy of Dr. F. Pundsack, Director of the Johns–Manville Basic Research Department.

https://doi.org/10.1346/CCMN.1967.0150134 Published online by Cambridge University Press

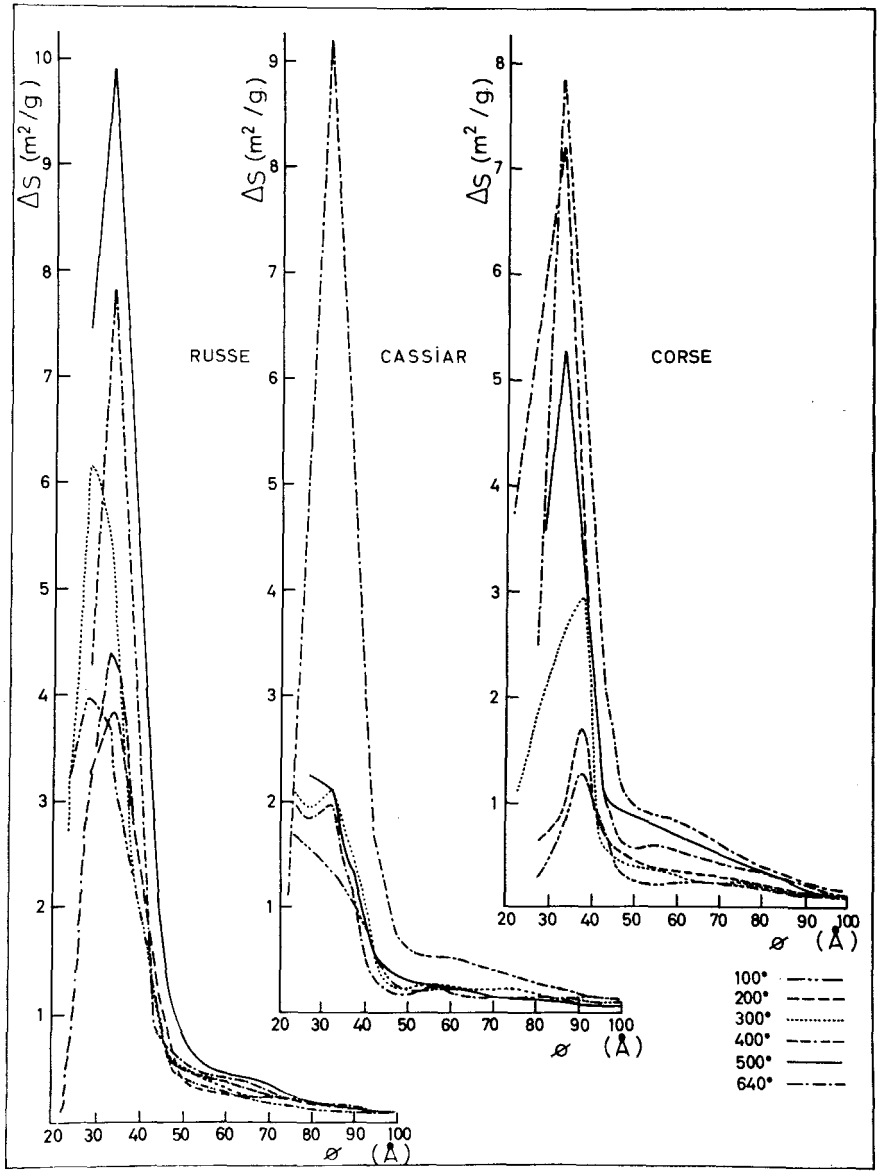


FIG. 6. Distribution function obtained for Russian, Cassiar, and Corsica chrysotiles.

https://doi.org/10.1346/CCMN.1967.0150134 Published online by Cambridge University Press

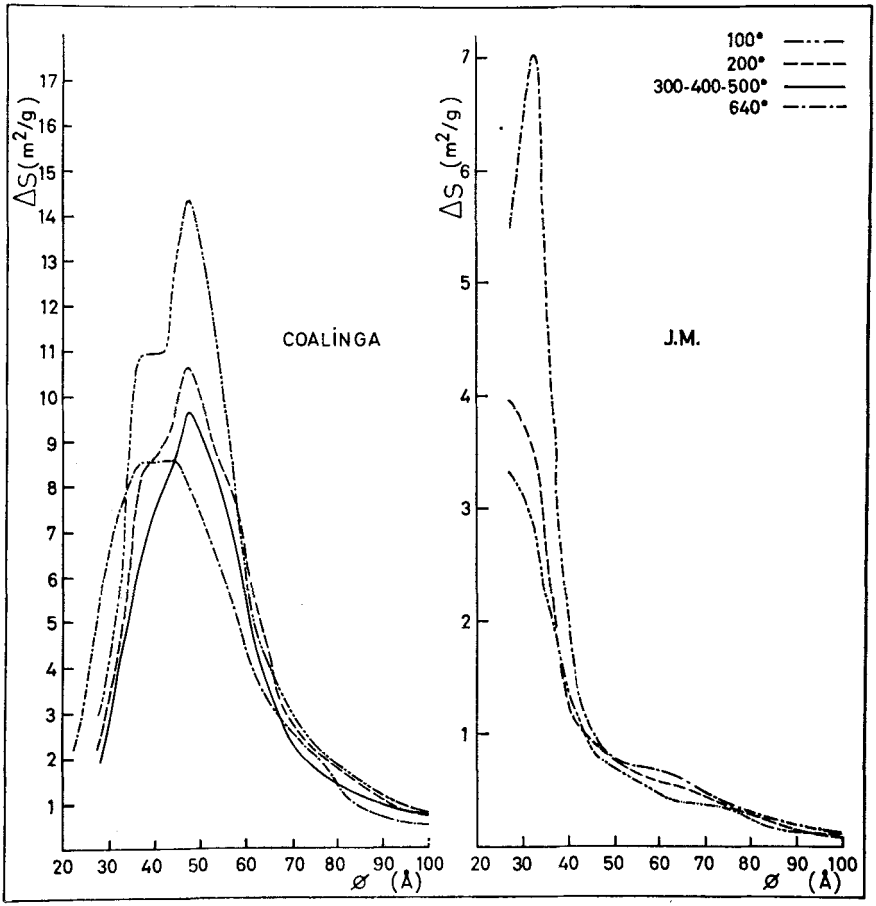


FIG. 7. Distribution functions obtained for Coalinga and J.M. chrysotiles.

WATER ADSORPTION ISOTHERMS

It was particularly interesting to check whether the increase of the specific surface areas measured with nitrogen was due to removal of hydration water molecules upon heating. This idea, already proposed by Young and Healey (1954), needs to be adapted to take account of the presence of amorphous materials, evidenced above.

Specific surface areas measured with water and obtained after pretreatment at 300°C are compared in Table 4 with the maximum specific surface areas measured with nitrogen after pretreatment in the range of 300° to 400°C.

https://doi.org/10.1346/CCMN.1967.0150134 Published online by Cambridge University Press

TABLE 4.—SURFACE AREAS (S, m^2g^{-1}) ACCESSIBLE TO N_2 AND H_2O MOLECULES AND CORRESPONDING PERCENTAGE VOID VOLUMES (ε, %)

Fiber	$S(N_2)$	$S(H_2O)$	$\varepsilon(N_2)$	$\varepsilon(H_2O)$
Arizona	17.6	18.4	1.82	—
J.M.	18.4	15.0	4.10	3.7
Russian	21.0	13.8	4.61	3.45
Corsica	17	—	3.27	5.58
Cassiar	14.3	12.3	2.83	3.12
Advocate	21.2	23.6	4.90	5.97
Coalinga	53.4	94.4	19.30	22.0

The general agreement is rather good but the most amazing discrepancy is that observed for Coalinga. It may be easily explained by taking into account that polar molecules have access to void spaces not available to non-polar molecules (Escard, 1950). Consider, in Fig. 2, the spaces (in black) not accessible to N_2 for energetic reasons, the cohesion energy of two close surfaces being higher than the van der Waals energy involved in the nitrogen adsorption process. In equation (1), the contribution of this region to the surface area of the external pore is given by $6\alpha RL$. For polar molecules, this negative term cancels and S^* becomes $2/R(1-r^2/R^2)\delta$. The computation of the specific surface area from equation (7) with this new S^* value has been performed using the characteristic textural parameters determined for Coalinga. As a result, the theoretical specific surface area increases from 51.3 m^2 to 89.5 m^2/g, the latter value being in good agreement with the area available to H_2O (Table 4).

It may be therefore concluded: (1) that outgassing chrysotile fibers at 300°C removes hydration water with the consequence that the "nitrogen" surface area increases; (2) that this increase is a function of the presence of amorphous materials; and (3) that there are regions which are not accessible to nitrogen for energetic reasons.

In Table 4, the percentage void volumes obtained from nitrogen and water adsorption isotherms are compared. Except for Coalinga where the quoted values are rather high, the other ones are very low, in good agreement with data given by Pundsack (1961). Void volume percentages in the range of a few per cent strongly suggest the presence of amorphous materials filling the porous system to variable extent while the values obtained for Coalinga are close to that estimated by Whittaker (1957) from electron micrographs, assuming emptied porous spaces.

CONCLUSIONS

The systematic study of nitrogen and water desorption isotherms applied to various chrysotiles leads to a model that fits reasonably well the observations made with other techniques such as electron microscopy and X-ray diffraction.

https://doi.org/10.1346/CCMN.1967.0150134 Published online by Cambridge University Press

The ideal arrangement of individual fibers in hexagonal close packing, with emptied internal and external pores, allows one to compute specific surface area, pore-size distribution function, and percentage void volume in good agreement with those observed in one case only, i.e. for Coalinga. It is interesting to point out that the deposit in which this fiber is found is quite remarkable since the chrysotile mineral is not interstratified with serpentine, as usual. Of course, this suggests a peculiar formation process that might be responsible for the different habit of Coalinga fibers.

For the other samples, the internal and probably also the external pores are filled to an appreciable extent by materials with chemical compositions similar to the bulk. From the percentage void volumes, the degree of filling is estimated to be of the order of magnitude of 50%, or higher. The pore-size distribution function does not permit one to compute this figure. The presence of one single maximum in this function suggests that the fiber distribution with respect to the outside diameter is nearly gaussian and that the radius of the internal cylindrical pore is either roughly proportional to the outside radius, or almost constant.

The most probable outside diameter can be derived from the most probable apparent pore diameter corresponding to the maximum observed in the pore-size distribution function. The outside diameters obtained in that way are in good agreement with those derived directly from electron micrographs.

The degree of filling by amorphous materials and the outside diameter appear to be characteristic of each chrysotile deposit. For samples with a high degree of filling, the hydration water cannot be driven off, unless they are pretreated between 300° and 400°C.

ACKNOWLEDGMENTS

One of us (M. della Faille) is indebted to Eternit S.A. for the financial support which has made this study possible.

Discussions with Dr. Pundsack from Johns–Manville Research Center have been very helpful. We want to acknowledge also the part taken by Drs. Marechal and Cahen from Labofina S.A. in the realization of the continuous-flow method used for recording the pore-size distribution functions. Many thanks are due also to Professor Meinguet, Head of the Computer Center of the University, for the calculations performed on theoretical models.

REFERENCES

BATES, T. F. (1959) Morphology and crystal chemistry of 1:1 layer lattice silicates: *Amer. Min.* **44**, 78–114.

BATES, T. F., and COMER, J. J. (1959) Further observations on the morphology of chrysotile and halloysite: *Clays and Clay Minerals*, Proc. 6th Conf., Pergamon Press, New York, 237–48.

BATES, T. F., SAND, L. B., and MINK, J. F. (1950) Tubular crystal of chrysotile asbestos: *Science* **7**, 512–13.

https://doi.org/10.1346/CCMN.1967.0150134 Published online by Cambridge University Press

CAHEN, R., MARECHAL, J., DELLA FAILLE, M., and FRIPIAT, J. J. (1965) Pore-size distribution by a rapid, continuous-flow method: *Anal. Chem.* **37**, 133–7.

CRANSTON, R. W., and INKLEY, F. A. (1957) The determination of pore structure from nitrogen adsorption isotherms: *Adv. in Catalysis* **9**, 143–6, Academic Press, New York.

DELLA FAILLE, M., DE KIMPE, C., and FRIPIAT, J. J. (1966) Influence de la déshydroxylation sur la morphologie et la texture des chrysotiles: *Silicates Industriels* **31**, 460–73.

ESCARD, J. (1950) Influence de la déshydratation progressive sur l'aire de surface de montmorillonites: *Jour. Chimie Physique* **47**, 113–17.

FANKUCHEN, I., and SCHNEIDER, M. (1944) Low angle X-ray scattering from chrysotile: *Jour. Amer. Chem. Soc.* **66**, 500–1.

HEALEY, F. H., and YOUNG, G. L. (1954) The surface properties of chrysotile asbestos: *Jour. Phys. Chem.* **58**, 885–6.

MASER, M., RICE, R. V., and KLUG, H. P. (1960) Chrysotile morphology: *Amer. Min.* **45**, 680–8.

NOLL, W., and KIRCHER, H. (1950) Zur Morphologie des Chrysotil-Asbesten: *Naturwiss.* **37**, 540–1.

NOLL, W., and KIRCHER, H. (1951) Uber die Morphologie von Asbesten und ihren Zusammenhang mit der Kristal-Struktur: *Neues Jahrh. Min. Mh.* **10**, 219–40.

NOLL, W., and KIRCHER, H. (1952) Veranderung von Chrysotil-Asbest im Electronenmikroskop: *Naturwiss.* **39**, 188–91.

PUNDSACK, F. L. (1956) The density and structure of chrysotile asbestos: *Jour. Phys. Chem.* **60**, 361–4.

PUNDSACK, F. L. (1961) The pore structure of chrysotile asbestos: *Jour. Phys. Chem.* **65**, 30–3.

TURKEVICH, J., and HILLIER, J. (1949) Electron microscopy on colloidal systems: *Anal. Chem.* **21**, 475–85.

WHITTAKER, E. J. W. (1957) The structure of chrysotile. V. Diffuse reflections and fibers texture: *Acta Cryst.* **10**, 149.

YOUNG, G. J., and HEALEY, F. H. (1954) The physical structure of asbestos: *Jour. Phys. Chem.* **58**, 881–4.

https://doi.org/10.1346/CCMN.1967.0150134 Published online by Cambridge University Press